Appendix B

Dispersion relations, analyticity, and unitarity of the scattering amplitude

Our analysis of high energy scattering amplitudes cannot be complete, since the problem of quark (and gluon) confinement in QCD has not been solved. It is clear that the solution of this problem lies beyond the realm of perturbative QCD. At the same time, nonperturbative physics may affect the scattering amplitudes (though maybe to a lesser extent than one would naively expect, since the saturation dynamics described in this book tends to suppress nonperturbative effects). Therefore, it would be very instructive to summarize the properties of the scattering amplitudes in the perturbative and nonperturbative approaches to any field theory.

First, any scattering amplitude should be a relativistic invariant (a scalar with respect to Lorenz transformations) and, because of this, it can depend only on variables that are relativistic invariants, namely on quantities such as $(p_i - p_j)^2$, where p_i^μ and p_j^μ are the four-momenta of external lines labeled i and j. In the case of a $2 \to 2$ scattering amplitude we have three such invariants, given by the Mandelstam variables (Mandelstam 1958)

$$\begin{aligned} s &= (p_A + p_B)^2 = m_A^2 + m_B^2 + 2 p_B \cdot p_A, \\ u &= (p_C - p_B)^2 = m_C^2 + m_B^2 - 2 p_C \cdot p_B, \\ t &= (p_A - p_C)^2 = m_C^2 + m_A^2 - 2 p_C \cdot p_A, \end{aligned} \tag{B.1}$$

with

$$s + u + t = m_A^2 + m_B^2 + m_C^2 + m_D^2. \tag{B.2}$$

The process is illustrated in the left-hand panel of Fig. B.1, where the notation is explained as well.

The second basic principle is the unitarity of the S-matrix: $S^\dagger S = I$ where I is the identity operator. This translates into the following equation for the T-matrix, defined by $S = I + iT$:

$$i(T^\dagger - T) = T^\dagger T. \tag{B.3}$$

Below we will rewrite Eq. (B.3) as a condition on scattering amplitudes.

The presentation of the material in this appendix is based mainly on the books Chew (1961, 1966), Roman (1969), Schweber (1961), and Weinberg (1996), vol. 1.

B.1 Crossing symmetry and dispersion relations

It turns out that when calculating any amplitude using Feynman diagrams in a field theory one always obtains a function that is analytic in its Lorentz-invariant arguments. In the case of a

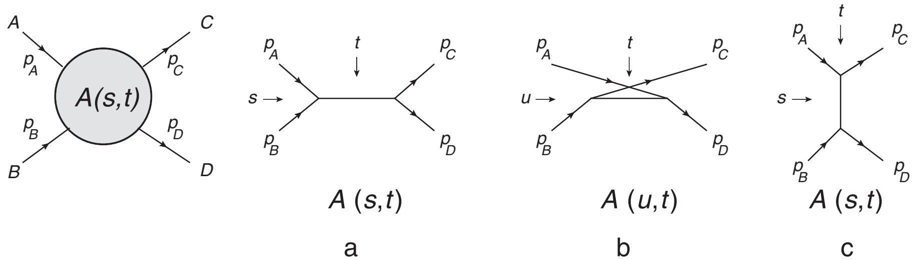

Fig. B.1. Scattering amplitude for a $2 \to 2$ process and tree-level diagrams for the process in the ϕ^3 theory in three different channels, s, u, and t, corresponding respectively to parts a, b, and c of the figure.

$2 \to 2$ scattering amplitude these arguments are the Mandelstam variables s, t, u. The singularities of the scattering amplitude are located only at the real values of these Lorentz-invariant variables. These singularities are closely related to the physical processes: they correspond to the production thresholds for physical particles (this is known as the Landau principle (Landau 1959, 1960)).

Relations between the scattering amplitudes for different processes may be obtained using *crossing symmetry*. This symmetry allows one to use only one function (say $A\,(s,t)$) to describe three different processes: $A + B \to C + D$, in the kinematic region where $s > 0$ and $t < 0$; $\bar{C} + B \to \bar{A} + D$, for $u > 0$ and $t < 0$; and $A + \bar{C} \to B + \bar{D}$, for $t > 0$ and $s < 0$. (Here $\bar{C}$, $\bar{D}$, and $\bar{A}$ denote antiparticles in complex-field theories and particles in real-field theories: in both cases the four-momenta are inverted under crossing symmetry transformations, e.g., $p^\mu_{\bar{A}} = -p^\mu_A$.)

The crossing symmetry can be illustrated using the example of simple tree-level graphs in ϕ^3 theory with the Lagrangian of Eq. (1.71). In Figs. B.1 a, b, c we plot the diagrams for the s-, t- and u-channel contributions respectively, all corresponding to the same process $A + B \to C + D$. Indeed, the diagrams of Fig. B.1 lead to the following expressions for the scattering amplitudes:

$$
\begin{aligned}
A(s,t;\text{Fig. B1a}) &= \frac{\lambda^2}{m^2 - (p_A + p_B)^2 - i\epsilon} = \frac{\lambda^2}{m^2 - s - i\epsilon} \\
A(u,t;\text{Fig. B1b}) &= \frac{\lambda^2}{m^2 - (-p_C + p_B)^2 - i\epsilon} = \frac{\lambda^2}{m^2 - u - i\epsilon} \\
A(t,s;\text{Fig. B1c}) &= \frac{\lambda^2}{m^2 - (p_A + -p_C)^2 - i\epsilon} = \frac{\lambda^2}{m^2 - t - i\epsilon}.
\end{aligned}
\tag{B.4}
$$

It is clear that Fig. B.1a describes the process $A + B \to C + D$, while the diagram of Fig. B.1b can be viewed either as describing the same process as the diagram of Fig. B.1a but with s replaced by $u = 4m^2 - s - t$ or it can be viewed as the tree-level diagram for the process $\bar{C} + B \to \bar{A} + D$, with the invariant s defined now as $s = (p_{\bar{C}} + p_B)^2$ if we assume that $p^\mu_{\bar{C}} = -p^\mu_C$. Defining

$$A(s,t) = A_{A+B\to C+D}\,(p_A, p_B, p_C, p_D) \tag{B.5}$$

we see that the relation between the amplitudes in diagrams Figs. B.1a, b that describes their crossing symmetry is

$$A_{\bar{C}+B\to\bar{A}+D}\,(p_{\bar{C}}, p_B, p_{\bar{A}}, p_D) = A_{A+B\to C+D}\,(-p_C, p_B, -p_A, p_D) = A(u,t). \tag{B.6}$$

https://doi.org/10.1017/9781009291446.012 Published online by Cambridge University Press

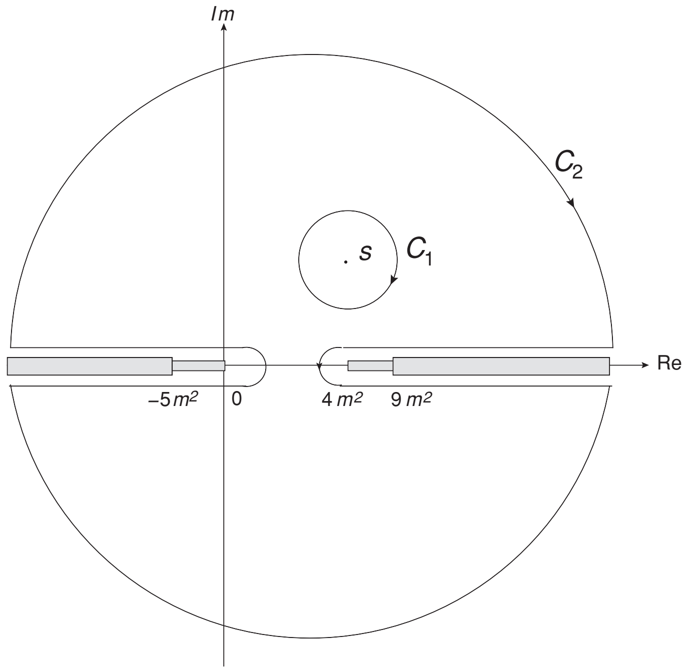

Fig. B.2. The singularities of the scattering amplitude $A(s,t)$, shown in the complex plane of the variable s. They are mainly given by branch cuts that start at the production thresholds for two, three, and more particles. For the sake of simplicity we do not show the pole contributions of Fig. B.1.

Similarly, for the amplitude resulting from the diagram Fig. B.1c we have

$$A_{A+\bar{C}\to B+\bar{D}}\,(p_A, p_{\bar{C}}, p_B, p_{\bar{D}}) = A_{A+B\to C+D}\,(p_A, -p_C, -p_B, p_D) = A(t,s). \tag{B.7}$$

Therefore, the scattering amplitude $A(s,t)$ as a function of the variables s and t is able to describe all three processes.

The analyticity of the scattering amplitude gives more detailed information about the amplitude. Indeed, owing to Cauchy's theorem the amplitude, being an analytical function, can be written in the form (see Fig. B.2)

$$A(s,t) = \frac{1}{2\pi i}\oint_{C_1} ds'\,\frac{A\big(s',t\big)}{s'-s} = \frac{1}{2\pi i}\oint_{C_2} ds'\,\frac{A\big(s',t\big)}{s'-s}. \tag{B.8}$$

The contours C_1 and C_2 are shown in Fig. B.2, and s is taken somewhere in the complex plane away from the real axis. The singularities of $A\,(s,t)$ are also shown in Fig. B.2: as mentioned before, they are confined to the real s-axis, and are typically branch cuts starting at the particle production thresholds. Since the amplitude does not have singularities at complex values of s, we can stretch the contour of integration C_1 to C_2 without modifying the value of the integral, as is reflected in Eq. (B.8). One can see that the integration over contour C_2 in Eq. (B.8) can be

https://doi.org/10.1017/9781009291446.012 Published online by Cambridge University Press

rewritten in the form

$$A(s,t) = \frac{1}{2\pi i}\left\{\int_{s_{min}}^{\infty} ds' \frac{\mathrm{Disc}_s\, A\big(s',t\big)}{s'-s} + \int_{u_{min}}^{\infty} du' \frac{\mathrm{Disc}_u\, A\big(u',t\big)}{u'-u}\right\}$$
$$+ \frac{1}{2\pi i} \oint_{\text{large circle}} ds' \frac{A\big(s',t\big)}{s'-s}, \tag{B.9}$$

where

$$\mathrm{Disc}_s A\left(s',t\right) = \lim_{\epsilon\to 0}\left[A\big(s'+i\epsilon,t\big) - A\big(s'-i\epsilon,t\big)\right] \tag{B.10}$$

and

$$\mathrm{Disc}_u A\left(u',t\right) = \lim_{\epsilon\to 0}\left[A\big(u'+i\epsilon,t\big) - A\big(u'-i\epsilon,t\big)\right]. \tag{B.11}$$

In the second term on the right-hand side of Eq. (B.9) we have changed the integration variable to $u' = 4m^2 - t - s'$; note that $A(u,t)$ is no longer equal to $A(s,t)$ with s replaced by u: rather $A(u,t) = A(s = 4m^2 - t - u, t)$. Typically the limits of integration in Eq. (B.9) would be $s_{min} = 4m^2$ and $u_{min} = 4m^2 - t$, and we are keeping t fixed and real. (If the amplitude has poles on the real axis for $0 < s < 4m^2$, as is the case for the ϕ^3-theory amplitudes given by Eq. (B.4), the contributions of such poles has to be included in the right-hand side of Eq. (B.9) by appropriately lowering s_{min}.)

The amplitude $A(s,t)$ has no imaginary part (no branch cuts corresponding to particle production) along the real axis between $s = 0$ (corresponding to $u = 4m^2, t = 0$) and $s = 4m^2$. Therefore it is a real function of s and t in this interval and, as can be shown, is in fact a real function of s and t in the whole region of its analyticity. We thus conclude that $A(s' - i\epsilon, t) = A^*(s' + i\epsilon, t)$, such that

$$\mathrm{Disc}_s\, A\big(s',t\big) = 2i\,\mathrm{Im}\, A(s,t)\,. \tag{B.12}$$

Similarly,

$$\mathrm{Disc}_u\, A\big(u',t\big) = 2i\,\mathrm{Im}\, A(u,t)\,. \tag{B.13}$$

(It should be stressed that, owing to the optical theorem, which follows from Eq. (B.3), Im $A(u,t)$ and Im $A(s,t)$ are directly related to physical processes.)

One can show that the contribution to the right-hand side of Eq. (B.9) coming from the integral over the large circle vanishes as we stretch the radius of the circle to infinity (see e.g. Weinberg (1996), vol. 1):

$$\frac{1}{2\pi i}\oint_{\text{large circle}} ds' \frac{A\big(s',t\big)}{s'-s} \longrightarrow 0. \tag{B.14}$$

Neglecting this last term on the right of Eq. (B.9) and employing Eqs. (B.12) and (B.13) we finally obtain the following *dispersion relation*:

$$A(s,t) = \frac{1}{\pi}\left\{\int_{s_{min}}^{\infty} ds' \frac{\mathrm{Im}_s\, A\big(s',t\big)}{s'-s} + \int_{u_{min}}^{\infty} du' \frac{\mathrm{Im}_u\, A\big(u',t\big)}{u'-u}\right\}. \tag{B.15}$$

Equation (B.15) allows one to reconstruct the full amplitude if its imaginary part is known.

https://doi.org/10.1017/9781009291446.012 Published online by Cambridge University Press

For example, the tree-level diagrams in Fig. B.1 yield

$$\mathrm{Im}_s\, A\big(s', t; \mathrm{Fig.\,B1a}\big) = \pi\lambda^2\delta\left(m^2 - s'\right), \tag{B.16a}$$

$$\mathrm{Im}_u\, A\big(u', t; \mathrm{Fig.\,B1b}\big) = \pi\lambda^2\delta\left(m^2 - u'\right). \tag{B.16b}$$

Substituting each of these imaginary parts into the right-hand side of Eq. (B.15) yields the appropriate amplitude after straightforward integration over the delta functions.

Note that a dispersion relation in the form Eq. (B.15) cannot be used in QCD since we know that QCD amplitudes grow as the energy s at large s (see e.g. Eq. (3.17)), making the integrals in Eq. (B.15) divergent. Therefore, we have to alter Eq. (B.15) by subtracting, for example, the amplitude $A(s = 0, t)$ obtained by putting $s = 0$ in Eq. (B.15). Doing this, we obtain the *subtracted dispersion relation*

$$\begin{aligned} A(s,t) = A(s=0,t) + \frac{1}{\pi}\Bigg\{ s\int_{s_{min}}^{+\infty} ds' \frac{\mathrm{Im}_s\, A\big(s',t\big)}{s'(s'-s)} \\ + [u - u(s=0)] \int_{u_{min}}^{+\infty} du' \frac{\mathrm{Im}_u\, A\big(u',t\big)}{[u' - u(s=0)](u'-u)} \Bigg\}. \end{aligned} \tag{B.17}$$

Finally, subtracting $s\partial_s A(s = 0, t)$ from Eq. (B.17) (with $A(s, t)$ again given by Eq. (B.15)) we obtain the *double-subtracted dispersion relation*

$$\begin{aligned} A(s,t) = A(s=0,t) + s\partial_s A(s=0,t) + \frac{1}{\pi}\Bigg\{ s^2\int_{s_{min}}^{+\infty} ds' \frac{\mathrm{Im}_s\, A\big(s',t\big)}{s'^2(s'-s)} \\ + [u - u(s=0)]^2 \int_{u_{min}}^{+\infty} du' \frac{\mathrm{Im}_u\, A\big(u',t\big)}{[u' - u(s=0)]^2(u'-u)} \Bigg\}. \end{aligned} \tag{B.18}$$

This is exactly the dispersion relation used in Eq. (3.43). Note that in perturbative QCD $A(s = 0, t) = 0$.

B.2 Unitarity and the Froissart–Martin bound

The unitarity constraint (B.3) can be written in terms of scattering amplitudes as (see e.g. Peskin and Schroeder (1995))

$$\begin{aligned} & M(k_1, k_2 \to k_1, k_2) - M^*(k_1, k_2 \to k_1, k_2) \\ & = i\sum_{n=2}^{\infty}\int\prod_{i=1}^{n}\frac{d^3q_i}{(2\pi)^3 2E_{q_i}}|M(k_1,k_2\to q_1,\ldots,q_n)|^2(2\pi)^4\delta^4\left(k_1+k_2-\sum_{j=1}^{n}q_j\right), \end{aligned} \tag{B.19}$$

where $M(k_1, k_2 \to q_1, \ldots, q_n)$ is the $2 \to n$ scattering amplitude for the scattering of two particles with momenta k_1, k_2 into n particles with momenta $q_1, \ldots, q_n$, and $M(k_1, k_2 \to k_1, k_2)$ is the forward scattering amplitude; E_{q_i} is the energy of a particle with momentum q_i.

Let us consider the case of high energy scattering, where k_1^+ and k_2^- are very large and so are $q_1^+ \approx k_1^+$ and $q_2^- \approx k_2^-$. Separating the *elastic* $2 \to 2$ contribution from the *inelastic* contributions ($2 \to 3$, $2 \to 4$, etc.) on the right-hand side of Eq. (B.19), and integrating over the delta-function in that contribution, yields

$$2\,\mathrm{Im}\, A(k_1, k_2 \to k_1, k_2) = \int \frac{d^2q_\perp}{(2\pi)^2}|A(k_1,k_2\to q_1,q_2)|^2 + \text{inelastic terms}, \tag{B.20}$$

where q is the momentum transfer four-vector, defined by

$$q = q_1 - k_1 = k_2 - q_2, \tag{B.21}$$

and we also define a new rescaled scattering amplitude

$$A(k_1, k_2 \to q_1, q_2) \equiv \frac{M(k_1, k_2 \to q_1, q_2)}{2\sqrt{2E_{k_1} 2E_{k_2} 2E_{q_1} 2E_{q_2}}} \approx \frac{M(k_1, k_2 \to q_1, q_2)}{2k_1^+ k_2^-}. \tag{B.22}$$

Since both the incoming and outgoing particles are on mass shell the momentum transfer q has only two free components, which we choose to be transverse and over which we integrated in Eq. (B.20).

The optical theorem then states that the total scattering cross section is given by (again, see e.g. Peskin and Schroeder (1995))

$$\sigma_{tot} = 2\,\mathrm{Im}\, A(k_1, k_2 \to k_1, k_2) \tag{B.23}$$

so that Eq. (B.20) simply implies that

$$\sigma_{tot} = \sigma_{el} + \sigma_{inel}, \tag{B.24}$$

where σ_{el} is the elastic $2 \to 2$ cross section and σ_{inel} is the total inelastic cross section.

As we have seen above, in general the elastic amplitude $A(k_1, k_2 \to q_1, q_2)$ can be written as a function of the Mandelstam variables s and t. However, for our purposes it is convenient to go to impact parameter ($\vec{b}_\perp$) space, using

$$A(k_1, k_2 \to q_1, q_2) = \int d^2b\, e^{-i\vec{q}_\perp \cdot \vec{b}_\perp} A(s, \vec{b}_\perp), \tag{B.25}$$

which, when applied in Eq. (B.20) yields

$$2\,\mathrm{Im}\, A(s, \vec{b}_\perp) = |A(s, \vec{b}_\perp)|^2 + \text{inelastic terms}. \tag{B.26}$$

In arriving at Eq. (B.26) we have used the fact that the forward amplitude corresponds to the case of zero momentum transfer, $t = 0$, or, equivalently, $q_\perp = 0$, such that

$$A(k_1, k_2 \to k_1, k_2) = \int d^2b\, A(s, \vec{b}_\perp). \tag{B.27}$$

Note that the total cross section in impact parameter space is

$$\sigma_{tot} = 2 \int d^2b\, \mathrm{Im}\, A(s, \vec{b}_\perp). \tag{B.28}$$

We also see immediately from Eq. (B.26) that the elastic cross section is given by

$$\sigma_{el} = \int d^2b\, |A(s, \vec{b}_\perp)|^2. \tag{B.29}$$

Relating the inelastic terms in Eq. (B.26) to the corresponding cross section yields

$$2\mathrm{Im}A(s, \vec{b}_\perp) = |A(s, \vec{b}_\perp)|^2 + \frac{d\sigma_{inel}}{d^2b}. \tag{B.30}$$

The simple nonnegativity condition

$$\frac{d\sigma_{inel}}{d^2b} \geq 0 \tag{B.31}$$

used in Eq. (B.30) yields

$$\mathrm{Im}\, A(s, \vec{b}_\perp) \leq 2. \tag{B.32}$$

This is an important condition, which follows from unitarity. When used in Eq. (B.28) it yields an upper bound for the total cross section:

$$\sigma_{tot} = 2\int d^2b\, \mathrm{Im}A(s, \vec{b}_\perp) \le 4\int d^2b = 4\pi R^2, \tag{B.33}$$

where R is the radius of the region in $b_\perp$-space where the interactions are sufficiently strong (the radius of the "black disk").

Parametrizing the forward scattering amplitude by (as follows from $S = I + iT$)

$$A(s, \vec{b}_\perp) = i\Big[1 - S(s, \vec{b}_\perp)\Big], \tag{B.34}$$

with $S(s, \vec{b}_\perp)$ the forward matrix element of the S-matrix, we see that the constraint (B.32) and the nonnegativity of the total cross section σ_{tot} together lead to $|\mathrm{Re}S(s, \vec{b}_\perp)| \le 1$.

Using Eq. (B.34) in Eqs. (B.28), (B.29), and (B.30) yields

$$\sigma_{tot} = 2\int d^2b\, \Big[1 - \mathrm{Re}\, S(s, \vec{b}_\perp)\Big], \tag{B.35a}$$

$$\sigma_{el} = \int d^2b\, \Big|1 - S(s, \vec{b}_\perp)\Big|^2, \tag{B.35b}$$

$$\sigma_{inel} = \int d^2b\, \Big[1 - |S(s, \vec{b}_\perp)|^2\Big]. \tag{B.35c}$$

In high energy scattering the bound on the total cross section is even stronger than Eq. (B.33). At very high energies inelastic processes dominate, so that $\sigma_{inel} \ge \sigma_{el}$, which leads to

$$\mathrm{Re}\, S(s, \vec{b}_\perp) \ge 0. \tag{B.36}$$

With the help of Eq. (B.34) we obtain

$$\mathrm{Im}A(s, \vec{b}_\perp) \le 1, \tag{B.37}$$

which is a stronger constraint than (B.32). Equation (B.37) leads to

$$\sigma_{tot} = 2\int d^2b\, \mathrm{Im}\, A(s, \vec{b}_\perp) \le 2\pi R^2. \tag{B.38}$$

This is the bound used in the text in Eq. (3.112). (For a derivation of this result in nonrelativistic quantum mechanics see Landau and Lifshitz (1958), vol. 3, Chapter 131.) Using the estimate (3.115) for the typical interaction range, i.e.,

$$R = b^* \sim \frac{\Delta}{2m_\pi} \ln s, \tag{B.39}$$

in Eq. (B.38) yields the Froissart–Martin bound (3.116)

$$\sigma_{tot} \le \frac{\pi\,\Delta^2}{2m_\pi^2} \ln^2 s \tag{B.40}$$

(Froissart 1961, Martin 1969, Lukaszuk and Martin 1967).